Density Functional Study of the Retrocyclization of Norbornadiene and Norbornene Catalyzed by Fe^+

Michael L. McKee*

Contribution from the Department of Chemistry, Auburn University, Auburn, Alabama 36849

Received May 10, 2001

Abstract: In the presence of Fe^+ catalyst, the retro Diels−Alder reaction of norbornadiene (NBD) is predicted to be stepwise with an activation barrier of 18.8 kcal/mol, which is 3.1 kcal/mol lower than the concerted retro reaction. For norbornene (NBN), the Fe^+-catalyzed retro reaction is also calculated to be stepwise with an activation barrier of 24.9 kcal/mol, which is 8.5 kcal/mol lower than the uncatalyzed stepwise reaction but 3.8 kcal/mol higher than the concerted reaction. The intermediates from the NBD and NBN retro Diels−Alder reactions, $C_5H_6FeC_2H_2^+$ and $C_5H_6FeC_2H_4^+$, are predicted to have low activation barriers for ligand-to-ligand hydrogen transfers (through an iron−hydrido intermediate) to form $CpFeC_2H_3^+$ and $CpFeC_2H_5^+$ and, ultimately, vinyl- and ethyl-substituted cyclopentadiene−iron complexes, respectively. In contrast to $FeC_2H_2^+$ and $FeC_2H_4^+$, the lowest-energy pathways on the $C_5H_6FeC_2H_2^+$ and $C_5H_6FeC_2H_4^+$ potential energy surfaces involve only one multiplicity (quartet). The C_2H_2 and C_2H_4 complexes of $CpFe^+$ and $C_5H_6Fe^+$ are compared.

Introduction

The theoretical study of organometallic ion chemistry provides important insights into catalytic systems and may allow the design of more selective and benign catalysts in the future.[1−14] There are many examples of transition metal cations coordinating to organic substrates and promoting particular reaction pathways. For example, Fe^+ can promote the retrocyclization of norbornadiene (NBD) and norbornene (NBN) to form $CpFeC_2H_2^+$ and $CpFeC_2H_4^+$, respectively.[15]

It is also known that ligands can change the reactivity of a transition metal center. For example, the ligands C_5H_5 and C_5H_6 can bind tightly to a transition metal cation and alter the reactivity from the bare metal cation.[16−25]

The motivation of the present study is to investigate (Scheme 1):

1. retrocyclization reactions of NBD−Fe^+ and NBN−Fe^+,
2. dehydrogenation of $C_5H_6FeC_2H_4^+$ and hydrogenation of NBD−Fe^+,
3. hydrogen/deuterium scrambling in $C_5H_6Fe^+/C_2D_4$,
4. C_2H_2 and C_2H_4 bond energies to $CpFe^+$ and $C_5H_6Fe^+$,
5. reaction of $C_5H_6Fe^+ + C_2H_4$ and interpretation of CID spectrum.

Computational Methods

All geometries were fully optimized[26] within a given point group using density functional theory with the B3LYP choice of exchange and correlation functionals.[27] A 6-31G(d) basis set was used for carbon and hydrogen and a (22s/16p/4d/1f) primitive basis set contracted to (5s/4p/2d/1f) was used for iron.[28] This basis set contained two sets of Cartesian d-functions (six functions/iron) and one set of spherical f-functions (seven functions/iron) with an 0.8 exponent. Vibrational frequencies were calculated at the B3LYP/6-31G(d) level to determine the nature of the stationary points and to make zero-point and heat capacity corrections.

The spin state of the transition metal fragment is important in determining reactivity. For example, it is known that the reactivity of $Fe^+(^6D)$ is greater than $Fe^+(^4F)$.[29] In addition, some transition metal reactions start off on one potential energy surface (PES) and switch to another PES surface via spin−orbit coupling. Such a process is denoted

(1) Simões, J. A. M.; Beauchamp, J. L. *Chem. Rev.* **1990**, *90*, 629.
(2) Koch, W.; Hertwig, R. H. Density Functional Theory Applications to Transition Metal Problems. In *The Encyclopedia of Computational Chemistry*; Schleyer, P. v. R., Allinger, N. L., Clark, T., Gasteiger, J., Kollman, P. A., Schaefer, H. F., III; Schreiner, P. R., Eds.; John Wiley: Chichester, 1998.
(3) Niu, S.; Hall, M. B. *Chem. Rev.* **2000**, *100*, 353.
(4) Hu, Z.; Boyd, R. J. *J. Chem. Phys.* **2000**, *113*, 9393.
(5) Pidun, U.; Frenking, G. *Chem. Eur. J.* **1998**, *4*, 522.
(6) Frenking, G.; Fröhlich, N. *Chem. Rev.* **2000**, *100*, 717.
(7) Veldkamp, A.; Frenking, G. *J. Chem. Soc., Chem. Commun.* **1992**, 118.
(8) Mandix, K.; Johansen, H. *J. Phys. Chem.* **1992**, *96*, 7261.
(9) Russo, T. V.; Martin, R. L.; Hay, P. J. *J. Chem. Phys.* **1994**, *101* 7729.
(10) Bauschlicher, C. W.; Langhoff, S. R.; Partridge, H. Ab initio calculations applied to problems in metal ion chemistry. In *Organometallic Ion Chemistry*; Freiser, B. S., Ed.; Kluwer Academic Publishers: Dordrecht, 1996; pp 47−87.
(11) (a) Sodupe, M.; Bauschlicher, C. W. *Chem. Phys. Lett.* **1993**, *207*, 19. (b) Bauschlicher, C. W.; Sodupe, M. *Chem. Phys. Lett.* **1995**, *240*, 526.
(12) Barone, V.; Adamo, C.; Mele, F. *Chem. Phys. Lett.* **1996**, *290*, 290.
(13) Glukhovtsev, M. N.; Bach, R. D.; Nagel, C. J. *J. Phys. Chem. A* **1997**, *101*, 316.
(14) Wang, S. G.; Schwarz, W. H. E. *J. Chem. Phys.* **1998**, *109*, 7252.
(15) (a) MacMillan, D. K.; Rayes, R. N.; Peake, D. A.; Gross, M. L. *J. Am. Chem. Soc.* **1992**, *114*, 7801. (b) Schroeter, K.; Schalley, C. A.; Schröder, D.; Schwarz, H. *Helv. Chim. Acta* **1997**, *80*, 1205.
(16) Jacobson, D. B.; Freiser, B. S. *J. Am. Chem. Soc.* **1985**, *107*, 72.
(17) Jacobson, D. B. *J. Am. Chem. Soc.* **1989**, *111*, 1626.
(18) Dearden, D. V.; Beauchamp, J. L.; van Koppen, P. A. M.; Bowers, M. T. *J. Am. Chem. Soc.* **1990**, *112*, 9372.
(19) (a) Huang, Y.; Freiser, B. S. *J. Am. Chem. Soc.* **1990**, *112*, 5085. (b) Huang, Y.; Freiser, B. S. *J. Am. Chem. Soc.* **1993**, *115*, 737.
(20) Chen, Q.; Sioma, C.; Kan, S. Z.; Freiser, B. S. *Int. J. Mass Spectrom.* **1998**, *179/180*, 231.
(21) Bakhtiar, R.; Jacobson, D. B. *J. Am. Soc. Mass Spectrom.* **1996**, *7*, 938.
(22) Innorta, G.; Pontoni, L.; Torroni, S. *J. Am. Mass. Spectrom.* **1998**, *9*, 314.
(23) Ekeberg, D.; Uggerud, E. *Organometallics* **1999**, *18*, 40.
(24) Abd-El-Aziz, A. S.; Bernardin, S. *Coord. Chem. Rev.* **2000**, *203*, 219.
(25) Baranov, V.; Bohme, D. K. *Int. J. Mass Spectrom.* **2001**, *204*, 209.

10.1021/ja011165q CCC: $20.00 © 2001 American Chemical Society
Published on Web 09/01/2001

Scheme 1

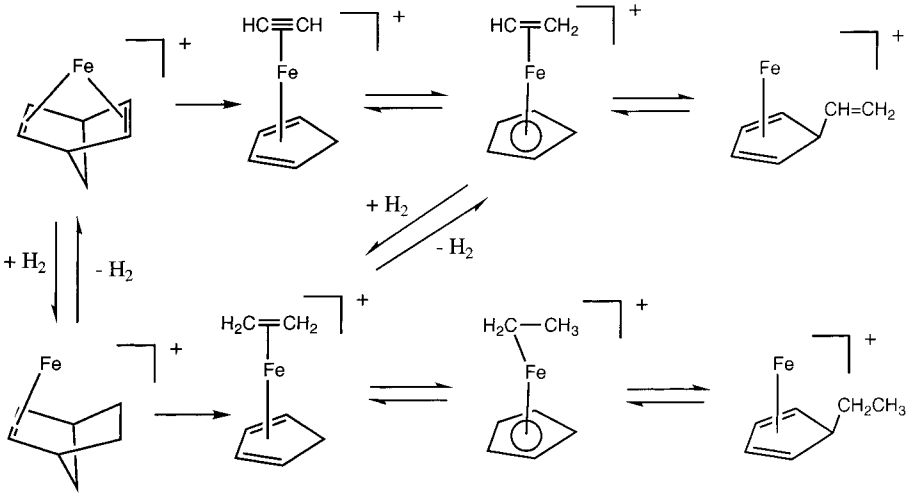

"two-state reactivity" (TSR) and has been suggested as a possibility in a number of Fe^+-R systems (Table 1).[30−38] The reactions under consideration here do not involve TSR. The quartet PES is lower in energy than the sextet and doublet surfaces for all geometries considered. The C_5H_6 and Cp ligands induce a ligand field at Fe^+ that reduces the spin-state to quartet for $C_5H_6Fe^+$ and quintet for $CpFe^+$, while complexation of C_2H_2 or C_2H_4 does not produce a sufficiently strong ligand field at the iron center to produce the doublet or triplet state. Thus, in the interaction of C_2H_2 and C_2H_4 with the bare Fe^+ cation, the complexes are sextets, while in the interaction of C_2H_2 and C_2H_4 with $C_5H_6Fe^+$, the complexes are quartets.

Total energies (hartrees) and zero-point energies (kcal/mol) are given in Table 2. Unless otherwise indicated, all reported energies will be enthalpies (298 K) at the B3LYP/6-31G(d) level. Enthalpies of reaction are given in Table 3 for hydrogenation, C_2H_2 addition, C_2H_4 addition, and Fe^+ addition reactions, where the boldface numbers correspond to the species designation in the figures and text.

Table 1. Comparison of Low-Spin/High-Spin Splitting of Fe^+-R with Fe^+-R and $CpFe^+-R$ Bond Dissociation Energies (BDE)

Fe^+-R	$\Delta E_{LS/HS}$ [a] (calcd)	Fe^+-R BDE (exptl)[b]	$CpFe^+-R$ BDE (calcd)[c]
Fe^+	−5.8[d]		
Fe^+-O	−18[e]		
Fe^+-S	−5.1[f]		
Fe^+-CH_4	−13.4[g]	13.7	
$Fe^+-C_2H_2$	19.6[h]	32	46.8
$Fe^+-C_2H_3$	−17.9[h]	56.8	62.0
$Fe^+-C_2H_4$	18.2[i]	34.7	43.2
$Fe^+-C_2H_5$	−14[j]	55.7	55.6
$Fe^+-C_2H_6$	<0[k]	15.2	
$Fe^+-C_2H_5SiH_3$	16.7[i]		
$Fe^+-C_5H_6$	12.1[c]		

[a] Sextet-quartet or quintet-triplet splitting in kcal/mol. A negative value indicates the high-spin species is lower in energy. [b] Table of Bond Energies. In *Organometallic Ion Chemistry*; Freiser, B. S., Ed., Kluwer Academic Publishers: Dordrecht, 1996, pp 283−332. [c] This work. [d] Experimental splitting of $Fe^+(^6D-^4F)$. Sugar, J.; Corliss, C. *J. Phys. Chem. Ref. Data* **1985**, *14*, 2 (suppl.). The 6-31G(d) basis set, used in this work, is too small to give a reasonable splitting for Fe^+. Adding diffuse functions (6-31+G(d)) gives a splitting of +2.3 kcal/mol, while a 6-311+G(d) basis set gives a splitting of +4.1 kcal/mol.[33] It is well-known that B3LYP artificially stabilizes $3d^n$ low-spin configurations relative to $3d^{n-1}4s$ high-spin configurations. [e] Reference 31. [f] Reference 32. [g] Reference 38. [h] Reference 35. [i] Reference 33. [j] Reference 36. [k] Reference 37.

Results and Discussion

1. Retrocyclization of NBD and NBN. Reaction profiles of the retrocyclization of NBD and NBN are given in Scheme 2, a and b, with molecular plots of stationary points given in Figure 1 (NBD) and Figure 2 (NBN). The values indicated above minima in Scheme 2, a and b, give the energy of the corresponding ligand plus Fe^+, $C_5H_6Fe^+$, or $CpFe^+$ (as appropriate) where energies (kcal/mol) are relative to $C_5H_6FeC_2H_2^+$ (**1**) or $C_5H_6FeC_2H_4^+$ (**7**). Thus, Fe^+ is bound to NBD by 67.1 kcal/mol (82.7−15.6, Scheme 2a). The C_s-symmetry $Fe-NBD^+$ complex (**6**) has two short Fe−C interactions (2.001 Å) and two long Fe−C interactions (2.349 Å). The C_{2v}-symmetry complex (not shown) is a transition state 6.3 kcal/mol above **6**. The initial transition state **TS5/6** (and the highest activation barrier, Scheme 2a), is reached when a C−C distance increases 1.546 → 2.358 Å with a corresponding reduction of the Fe−C distance 2.001 → 1.869 Å. The intermediate **5** is a bicyclic system where the iron has inserted into a C−C bond. From **5**, a transition state **TS1/5** is reached for breaking the

(26) Frisch, M. J.; Trucks, G. W.; Schlegel, H. B.; Scuseria, G. E.; Robb, M. A.; Cheeseman, J. R.; Zakrzewski, V. G.; Montgomery, J. A., Jr.; Stratmann, R. E.; Burant, J. C.; Dapprich, S.; Millam, J. M.; Daniels, A. D.; Kudin, K. N.; Strain, M. C.; Farkas, O.; Tomasi, J.; Barone, V.; Cossi, M.; Cammi, R.; Mennucci, B.; Pomelli, C.; Adamo, C.; Clifford, S.; Ochterski, J.; Petersson, G. A.; Ayala, P. Y.; Cui, Q.; Morokuma, K.; Malick, D. K.; Rabuck, A. D.; Raghavachari, K.; Foresman, J. B.; Cioslowski, J.; Ortiz, J. V.; Stefanov, B. B.; Liu, G.; Liashenko, A.; Piskorz, P.; Komaromi, I.; Gomperts, R.; Martin, R. L.; Fox, D. J.; Keith, T.; Al-Laham, M. A.; Peng, C. Y.; Nanayakkara, A.; Gonzalez, C.; Challacombe, M.; Gill, P. M. W.; Johnson, B.; Chen, W.; Wong, M. W.; Andres, J. L.; Gonzalez, C.; Head-Gordon, M.; Replogle, E. S.; Pople, J. A. *Gaussian 98*; Gaussian, Inc.: Pittsburgh, PA, 1998.

(27) See: (a) *The Encyclopedia of Computational Chemistry*; Schleyer, P. v. R., Allinger, N. L., Clark, T., Gasteiger, J., Kollman, P. A., Schaefer, H. F., III, Schreiner, P. R., Eds.; John Wiley: Chichester, 1998. (b) Koch, W.; Holthausen, M. C. *A Chemist's Guide to Density Functional Theory*; Wiley-VCH: Weinheim, 2000.

(28) Rassolov, V. A.; Pople, J. A.; Ratner, M. A.; Windus, T. L. *J. Chem. Phys.* **1998**, *109*, 1223.

(29) (a) Elkind, J. L.; Armentrout, P. B. *J. Am. Chem. Soc.* **1986**, *108*, 2765. (b) Armentrout, P. B. *Science* **1991**, *251*, 175.

(30) Schröder, D.; Shaik, S.; Schwarz, H. *Acc. Chem. Res.* **2000**, *33*, 139.

(31) Yoshizawa, K.; Shiota, Y.; Yamabe, T. *J. Chem. Phys.* **1999**, *111*, 538.

(32) Bärsch, S.; Schröder, D.; Schwarz, H.; Armentrout, P. A. *J. Phys. Chem. A* **2001**, *105*, 2005.

(33) Bärsch, S.; Schröder, D.; Schwarz, H. *Int. J. Mass Spectrom.* **2000**, *202*, 363.

(34) Klippenstein, S. J.; Yang, C.-N. *Int. J. Mass Spectrom.* **2000**, *201*, 253.

(35) Chen, H.; Jacobson, D. B.; Freiser, B. S. *Organometallics* **1999**, *18*, 5460.

(36) Fiedler, A.; Schröder, D.; Zummack, W.; Schwarz, H. *Inorg. Chim. Acta* **1997**, *259*, 227.

(37) Holthausen, M. C.; Fiedler, A.; Schwarz, H.; Koch, W. *Angew. Chem., Int. Ed. Engl.* **1995**, *34*, 2282.

(38) Musaev, D. G.; Morokuma, K. *J. Chem. Phys.* **1994**, *101*, 10697.

Table 2. Total Energies (hartrees), Zero-point Energies (kcal/mol), Heat Capacity Corrections (kcal/mol), and Entropies (cal/mol·K) Calculated at B3LYP/6-31G(d) Geometries

	PG	state	B3LYP/ 6-31G(d)	ZPE[a]	Cp(corr.)[b]	entropy
H_2	$D_{\infty h}$	$^1\Sigma_g^+$	−1.17548	6.36(0)	2.07	31.13
C_2H_2	$D_{\infty h}$	$^1\Sigma_g^+$	−77.32564	16.72(0)	2.43	48.18
C_2H_4	D_{2h}	^1A_g	−78.58746	32.15(0)	2.50	52.33
C_2H_6	D_{3d}	$^1A_{1g}$	−79.83042	47.22(0)	2.77	54.37
C_2H_3	C_s	$^2A'$	−77.90121	23.05(0)	2.54	55.83
C_2H_5	C_s	$^2A'$	−79.15787	37.43(0)	3.07	61.09
C_5H_5	C_{2v}	$^2A_2$	−193.46232	49.04(1)	3.07	65.82
C_5H_6	C_{2v}	$^1A_1$	−194.10106	58.29(0)	3.19	65.31
C_7H_8	C_{2v}	$^1A_1$	−271.47728	80.92(0)	3.64	70.02
C_7H_8 (TS)	C_s	$^1A'$	−271.39278	76.83(1)	4.46	76.80
$C_2H_3-C_5H_5$	C_s	$^1A'$	−271.49221	79.27(0)	4.58	79.20
C_7H_{10}	C_s	$^1A'$	−272.72738	96.40(0)	3.86	72.98
C_7H_{10} (TS)	C_s	$^1A'$	−272.65674	92.81(1)	4.44	76.98
$C_2H_5-C_5H_5$	C_1	^1A	−272.72813	94.22(0)	4.58	79.20
Fe^+	K	^6D	−1263.23744	0.00	1.48	43.14[c]
$CpFe^+$	C_s	$^5A'$	−1456.84089	52.03(1)	3.44	74.88
$CpFeH^+$	C_s	$^4A''$	−1457.41517	56.21(0)	4.30	79.48
$C_5H_6Fe^+$	C_s	$^4A''$	−1457.42428	59.06(0)	4.02	78.04
$C_5H_6Fe^+$	C_s	$^6A''$	−1457.40528	58.90(0)	4.34	81.94
1	C_1	^4A	−1534.84279	77.67(0)	6.03	94.59
1′	C_s	$^4A''$	−1534.84272	77.62(1)	5.51	90.06
TS1/2	C_1	^4A	−1534.81603	74.74(1)	5.75	91.73
2	C_s	$^4A'$	−1534.81997	75.20(1)	5.64	90.50
TS2/3	C_s	$^4A'$	−1534.81933	74.82(1)	5.90	94.53
3	C_1	^4A	−1534.84505	77.77(0)	5.93	93.79
TS3/4	C_1	^4A	−1534.82480	78.61(1)	5.24	88.32
4	C_1	^4A	−1534.85005	80.46(0)	5.06	85.74
TS1/5	C_1	^4A	−1534.79869	78.45(1)	5.08	86.07
5	C_1	^4A	−1534.82003	79.92(0)	5.20	87.36
TS5/6	C_1	^4A	−1534.78877	79.71(1)	4.49	81.91
6	C_s	$^4A''$	−1534.82206	81.66(0)	4.59	83.28
6(TS)	C_{2v}	$^4B_2$	−1534.81039	81.02(1)	4.28	79.71
7	C_1	^4A	−1536.09597	93.03(0)	6.24	96.93
7′	C_s	$^4A''$	−1536.08942	92.32(1)	6.03	97.24
TS7/7	C_1	^4A	−1536.05471	90.91(1)	6.06	95.10
TS7/8	C_1	^4A	−1536.07371	90.53(1)	5.87	92.56
8	C_s	$^4A'$	−1536.07415	91.14(0)	6.19	96.04
TS8/9	C_1	^4A	−1536.07372	90.73(1)	5.89	94.88
9	C_s	$^4A'$	−1536.09214	92.94(0)	6.03	95.03
TS9/10	C_1	^4A	−1536.04992	94.09(1)	5.40	89.08
10	C_1	^4A	−1536.07201	94.90(0)	5.49	89.18
10′	C_s	$^4A''$	−1536.07006	94.27(1)	5.25	87.39
TS7/11	C_1	^4A	−1536.01539	87.35(1)	6.25	97.01
11	C_1	^4A	−1536.03142	88.31(0)	6.74	99.82
TS7/12	C_1	^4A	−1536.03899	93.84(1)	5.18	86.78
12	C_1	^4A	−1536.05386	94.61(0)	5.56	90.86
TS12/13	C_1	^4A	−1536.00849	94.28(1)	4.83	84.61
13	C_s	$^4A''$	−1536.05164	96.24(0)	5.04	89.23
TS13/14	C_1	^4A	−1536.01393	92.66(1)	4.90	85.12
14	C_1	^4A	−1536.02160	92.90(0)	5.12	86.27
TS14/15	C_1	^4A	−1535.98579	90.28(1)	4.64	82.73
15	C_s	$^4A''$	−1536.02152	90.89(0)	5.52	88.61
$CpFeC_2H_2^+$	C_s	$^5A'$	−1534.24414	70.70(0)	5.79	93.62
$CpFeC_2H_2^+$	C_1	^3A	−1534.23958	71.24(0)	5.60	91.96
$CpFeC_2H_2^+$	C_s	$^3A''$	−1534.23956	71.19(1)	5.05	85.89
$CpFeC_2H_4^+$	C_s	$^5A'$	−1535.50094	86.50(0)	5.93	95.22
$CpFeC_2H_4^+$	C_1	^3A	−1535.48532	86.59(0)	5.75	91.13
$CpFeC_2H_4^+$	C_s	$^3A''$	−1535.47846	85.76(2)	5.12	86.36

[a] Zero-point energies with number of imaginary frequencies in parentheses. [b] Heat capacity and thermal corrections to 298 K. [c] Entropy for Fe atom taken from http://webbook.nist.gov/chemistry.

second C−C bond in which the Fe center begins to form a π complex with the nascent C_2H_2 ligand. The $C_5H_6FeC_2H_2^+$ complex (**1**) is 15.6 kcal/mol more stable than the NBD−Fe^+ complex (**6**).

From **1**, a shallow hydrido complex $CpFe(H)C_2H_2^+$ (**2**) is formed, 11.5 kcal/mol less stable than **1**. In the transition state (**TS1/2**), the forming Fe−H distance is 1.565 Å, and the breaking C−H distance is 1.792 Å. The hydrido ligand in **2** is transferred to the C_2H_2 ligand in transition state **TS2/3** to form the $CpFeC_2H_3^+$ complex **3**. Finally, the C_2H_3 ligand can add to the cyclopentadienyl ligand to form **4**, in which a vinylcyclopentadiene ligand is complexed to Fe^+. The vinyl group in **4** has twisted to allow the iron center to form a π complex with Fe−C distances of 2.101 and 2.126 Å.

The C−C distance of the acetylenic ligand in **2** gradually increases to the C−C distance in the vinyl substitutent of **4** (1.253 → 1.330 → 1.391 Å). The products **3** and **4** are 1.4 and 2.7 kcal/mol more stable than **1**, respectively.

The reaction profile of Fe^+ with NBN (Scheme 2b) is similar to that of Fe^+ with NBD (Scheme 2a). The Fe^+ interacts strongly with the double bond (**13**, Fe−C 2.011; C−C 1.428 Å). As the C−C bond breaks in **TS12/13**, the Fe^+ center approaches the carbon atom (Fe−C 1.996 Å) and is stabilized by an agostic

Table 3. Reaction Enthalpies (kcal/mol) at 298 K at the B3LYP/6-31G(d) Level for Various Reactions

reaction	ΔH_{rxn}
Hydrogenation	
$C_2H_2 + H_2 \rightarrow C_2H_4$	−47.1
$C_2H_3 + H_2 \rightarrow C_2H_5$	−44.5
$C_2H_3-C_5H_5 + H_2 \rightarrow C_2H_5-C_5H_5$	−31.1
$C_7H_8 + H_2 \rightarrow C_7H_{10}$	−39.6
$CpFeC_2H_2^+ + H_2 \rightarrow CpFeC_2H_4^+$	−37.0
$C_5H_6FeC_2H_2^+ + H_2 \rightarrow C_5H_6FeC_2H_4^+$ (**1/7**)	−41.6
$CpFeC_2H_3^+ + H_2 \rightarrow CpFeC_2H_5^+$ (**3/9**)	−38.1
$FeC_7H_8^+ + H_2 \rightarrow FeC_7H_{10}^+$ (**6/13**)	−27.3
$C_2H_3-C_5H_5Fe^+ + H_2 \rightarrow C_2H_5-C_5H_5Fe^+$ (**4/10**)	−22.7
$FeC_7H_8^+ + H_2 \rightarrow Fe(H_2)C_7H_8^+$ (**6/15**)	−13.3
$CpFeC_2H_3^+ + H_2 \rightarrow CpFe(H_2)C_2H_3^+$ (**3/11**)	−3.9
C_2H_2 Addition	
$C_5H_6 + C_2H_2 \rightarrow C_7H_8$	−27.8
$C_5H_6Fe^+ + C_2H_2 \rightarrow FeC_7H_8^+$ (**6**)	−41.2
$CpFe^+ + C_2H_2 \rightarrow CpFeC_2H_2^+$	−46.8
$CpFeH^+ + C_2H_2 \rightarrow CpFe(H)C_2H_2^+$ (**2**)	−48.5
$C_5H_6Fe^+ + C_2H_2 \rightarrow C_5H_6FeC_2H_2^+$ (**1**)	−56.8
C_2H_4 Addition	
$C_5H_6 + C_2H_4 \rightarrow C_7H_{10}$	−20.3
$C_5H_6Fe^+ + C_2H_4 \rightarrow FeC_7H_{10}^+$ (**13**)	−21.5
$CpFe^+ + C_2H_4 \rightarrow CpFeC_2H_4^+$	−43.2
$CpFeH^+ + C_2H_4 \rightarrow CpFe(H)C_2H_4^+$ (**8**)	−42.7
$C_5H_6Fe^+ + C_2H_4 \rightarrow C_5H_6FeC_2H_4^+$ (**7**)	−51.3
Fe^+ Addition	
$C_5H_6 + Fe^+ \rightarrow C_5H_6Fe^+$	−53.7
$Cp + Fe^+ \rightarrow CpFe^+$	−86.7
$C_7H_8 + Fe^+ \rightarrow FeC_7H_8^+$ (**6**)	−67.1
$C_7H_{10} + Fe^+ \rightarrow FeC_7H_{10}^+$ (**13**)	−54.9
$C_2H_3-C_5H_5 + Fe^+ \rightarrow C_2H_3-C_5H_5Fe^+$ (**4**)	−87.3
$C_2H_5-C_5H_5 + Fe^+ \rightarrow C_2H_5-C_5H_5Fe^+$ (**10**)	−67.0
Miscellaneous Addition	
$CpFe^+ + C_2H_3 \rightarrow CpFeC_2H_3^+$ (**3**)	−62.0
$CpFe^+ + C_2H_5 \rightarrow CpFeC_2H_5^+$ (**9**)	−55.6
$C_2H_2 + H \rightarrow C_2H_3$	−42.3
$C_2H_3 + H \rightarrow C_2H_4$	−109.1
$C_2H_4 + H \rightarrow C_2H_5$	−39.6
$C_2H_5 + H \rightarrow C_2H_6$	−100.1
$2C_2H_3 \rightarrow C_2H_2 + C_2H_4$	−66.8
$CpFeC_2H_2^+ + H \rightarrow CpFeC_2H_3^+$	−57.4
$CpFeC_2H_3^+ + H \rightarrow CpFeC_2H_4^+$	−90.4
$CpFeC_2H_4^+ + H \rightarrow CpFeC_2H_5^+$	−52.0
$2CpFeC_2H_3^+ \rightarrow CpFeC_2H_2^+ + CpFeC_2H_4^+$	−33.0

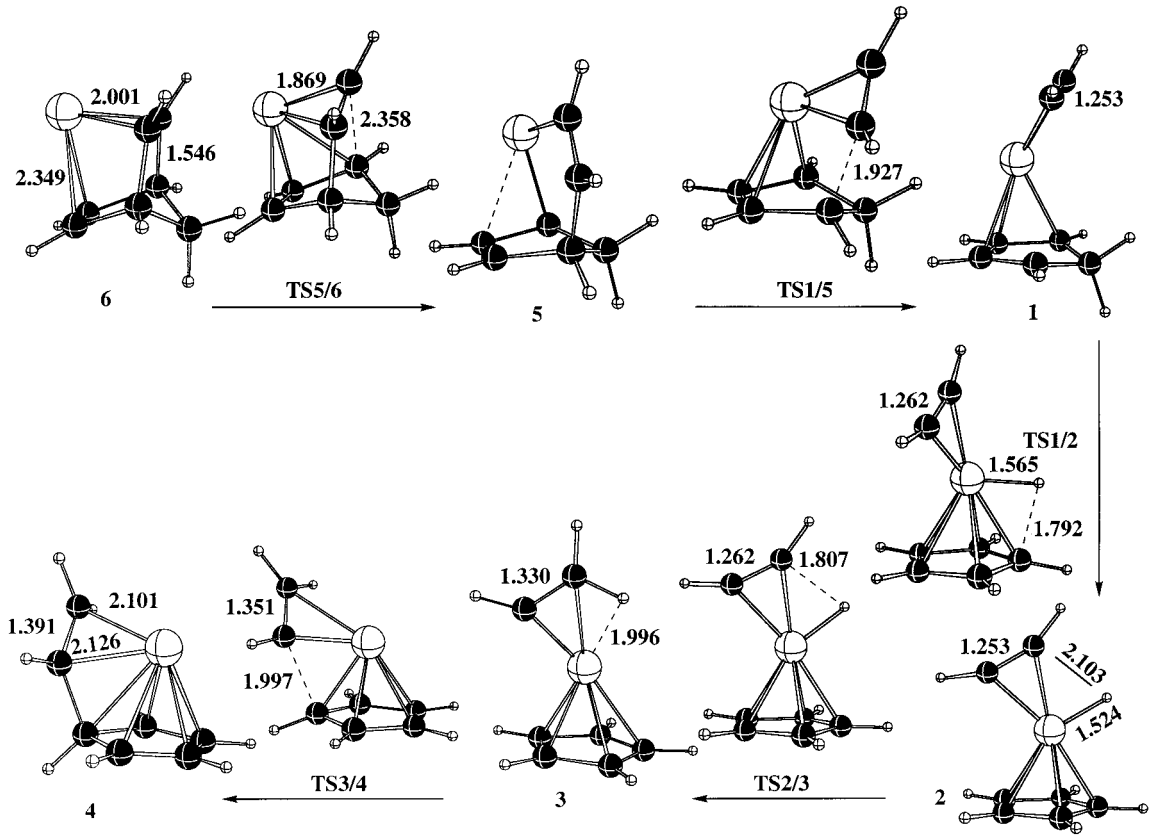

Figure 1. Molecular plots of species optimized at the B3LYP/6-31G(d) level. The reaction profile with energies in kcal/mol relative to C_5H_6-$FeC_2H_2^+$ (**1**) is given in Scheme 2a.

Scheme 2

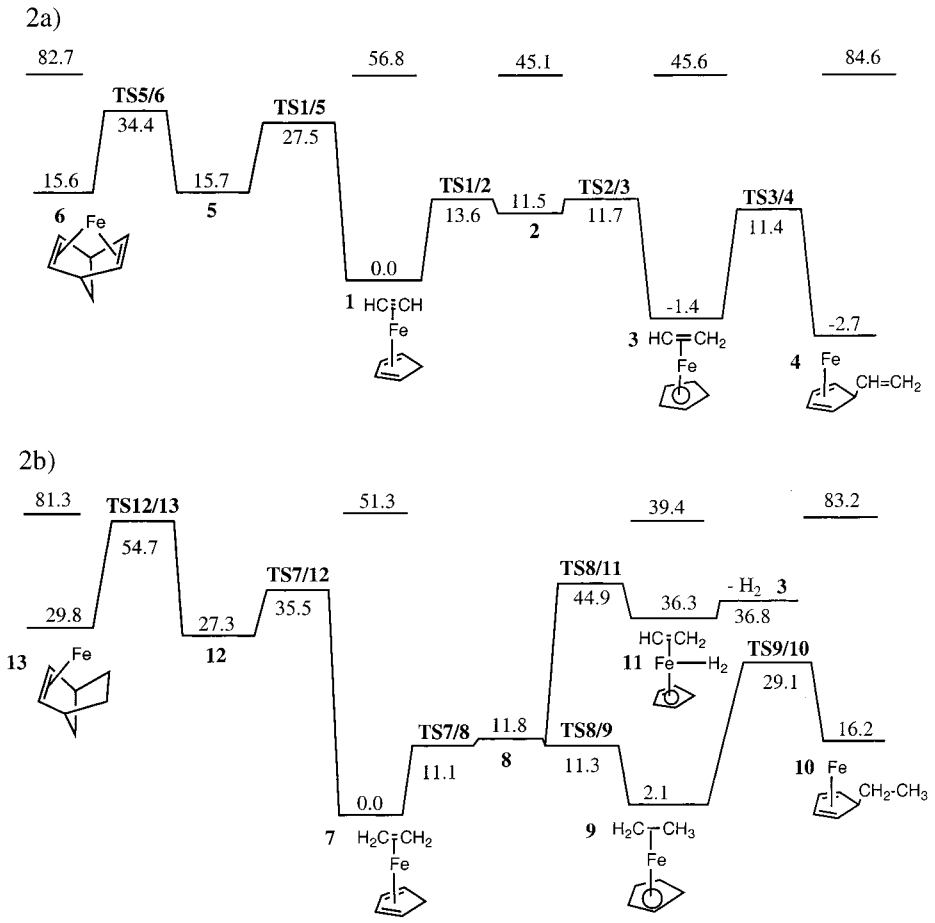

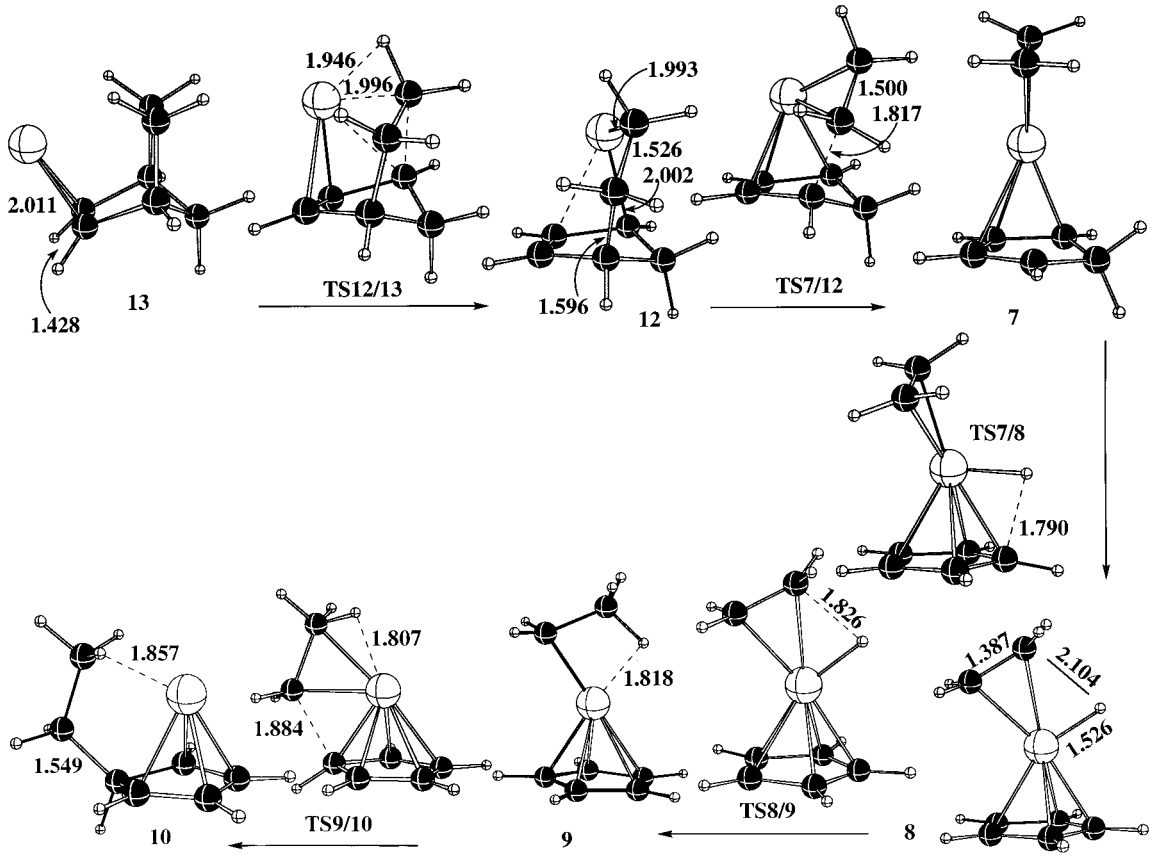

Figure 2. Molecular plots of species optimized at the B3LYP/6-31G(d) level. The reaction profile with energies in kcal/mol relative to C_5H_6-$FeC_2H_4^+$ (**7**) is given in Scheme 2b.

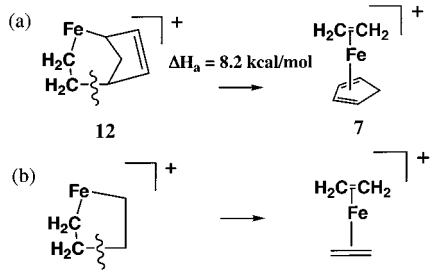

Figure 3. (a) Schematic of the bicyclic metallocycle **12** which can cleave a C−C bond with an activation barrier of 8.2 kcal/mol. (b) Schematic of the C−C bond cleavage in the iron cyclopentane cation, a very similar reaction, which is the which is thought to have a low barrier to C−C cleave to form $Fe(C_2H_4)_2^+$.

interaction (Fe−H 1.946 Å). The intermediate **12** is a bicyclic system with two short Fe−C distances (1.993 and 2.002 Å). The second C−C distance increase from 1.596 to 1.817 Å in **TS7/12** while the C−C distance in the nascent ethenic ligand decreases from 1.526 to 1.500 Å. The cleavage of the Fe−C bond in **12** bears some similarity to the cleavage of iron cyclopentane to $Fe(C_2H_4)_2^+$ (Figure 3) which has been studied by mass spectrometric methods.[39−43]

In the Fe^+-catalyzed retrocyclization of NBD and NBN, breaking the first C−C bond in NBD has a lower activation barrier (18.8 vs 24.9 kcal/mol) than the corresponding C−C bond in the NBN reaction, while breaking the second C−C bond has a higher activation barrier (11.8 vs 8.2 kcal/mol). Also, the reaction is less exothermic when R=C_2H_2 than when R=C_2H_4 (ΔH_{rxn} = −15.6 vs −29.8 kcal/mol). A comparison of the uncatalyzed[44] and Fe^+-catalyzed retrocyclization is made in Figure 4. For the retrocyclization of NBD, the barrier for the Fe^+-catalyzed reaction is 3.1 kcal/mol lower than the concerted uncatalyzed reaction. In contrast, the barrier for the retrocyclization of NBN is 3.8 kcal/mol higher by the Fe^+-catalyzed pathway compared to the uncatalyzed[44] concerted pathway. However, the Fe^+-catalyzed pathway is 8.5 kcal/mol lower than the uncatalyzed[44] two-step diradical pathway.

Relative to the $C_5H_6FeC_2H_4^+$ complex **7**, the hydrido intermediate $CpFe(H)C_2H_4^+$ **8** is 11.8 kcal/mol less stable. After zero-point and heat capacity corrections, the transitions states **TS7/8** and **TS8/9** are computed to be below the energy of the intermediate **8**, indicating that the hydrogen transfer between the Cp and C_2H_4 ligand takes place without the metal−hydrido intermediate.

The ring protonated ($C_5H_6FeC_2H_2^+$ and $C_5H_6FeC_2H_4^+$) and metal-protonated ($CpFe(H)C_2H_2^+$ and $CpFe(H)C_2H_4^+$) systems resemble protonated ferrocene,[45] where the ring- and metal-protonated forms are close in energy. At the highest level of

(39) Jacobson, D. B.; Freiser, B. S. *J. Am. Chem. Soc.* **1983**, *105*, 7492.
(40) Jacobson, D. B.; Freiser, B. S. *J. Am. Chem. Soc.* **1984**, *106*, 3900.
(41) Jacobson, D. B.; Freiser, B. S. *J. Am. Chem. Soc.* **1985**, *107*, 2605.
(42) Buckner, S. W.; Freiser, B. S. *Polyhedron* **1988**, *7*, 1583.
(43) Surya, P. I.; Roth, L. M.; Ranatunga, D. R. A.; Freiser, B. S. *J. Am. Chem. Soc.* **1996**, *118*, 1118.
(44) (a) Diau, E. W.-G.; De Feyter, S.; Zewail, A. H. *Chem. Phys. Lett.* **1999**, *304*, 134. (b) Beno, B. R.; Wilsey, S.; Houk, K. N. *J. Am. Chem. Soc.* **1999**, *121*, 4816. (c) Houk, K. N.; Wilsey, S. L.; Beno, B. R.; Kless, A.; Nendel, M.; Tian, J. *Pure Appl. Chem.* **1998**, *70*, 1947. (d) Lewis, D. K.; Glenar, D. A.; Hughes, S.; Kalra, B. L.; Schlier, J.; Shukla, R.; Baldwin, J. E. *J. Am. Chem. Soc.* **2001**, *123*, 996.
(45) (a) Mayor-López, M. J.; Lüthi, H. P.; Koch, H.; Morgantini, P. Y.; Weber, J. *J. Chem. Phys.* **2000**, *113*, 8009. (b) Karlsson, A.; Broo, A.; Ahlberg, A. *Can. J. Chem.* **1999**, *77*, 628. (c) Mayor-López, M. J.; Weber, J.; Mannfors, B.; Cunningham, A. F. *Organometallics* **1998**, *17*, 4983. (d) Klopper, W.; Lüthi, H. P. *Chem. Phys. Lett.* **1996**, *262*, 546. (e) Jungwirth, P.; Stussi, D.; Weber, J. *Chem. Phys. Lett.* **1992**, *190*, 29. (f) McKee, M. L. *J. Phys. Chem.* **1992**, *96*, 1683.

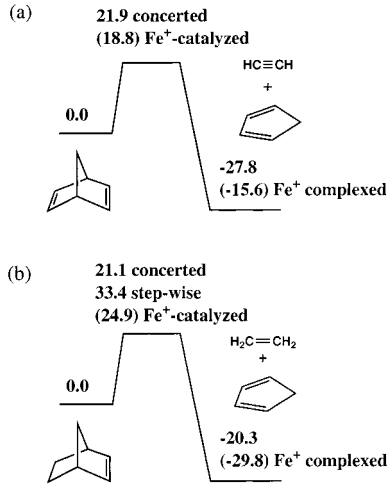

Figure 4. (a) Reaction profile of the retrocyclization of norbornadiene (NBD) where the Fe^+-catalyzed reaction is 3.1 kcal/mol lower than the concerted reaction. (b) Reaction profile of the retrocyclization of norbornene (NBN) where the Fe^+-catalyzed reaction is 3.8 kcal/mol higher than the concerted reaction, but 8.5 kcal/mol lower than the stepwise mechanism.

theory attempted to date (CCSD(T)/pVDZ//BPW91/6-311G), ring protonation of ferrocene is 2.1 kcal/mol more stable than metal protonation. The present results also find the ring-protonated forms ($C_5H_6FeC_2H_2^+$ and $C_5H_5FeC_2H_4^+$) to be more stable than metal-protonated forms by 11.5 and 11.8 kcal/mol, respectively.

Ginsberg et al.[46] were able to isolate both the metal−cyclopentadiene form (left) and the metal−hydrido-cyclopendienyl form (right) in a related rhodium system (see insert).

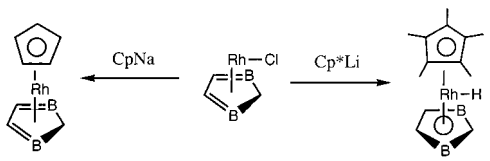

One of the hydrogens in the 2,3-dihydro-1,3-diborole ring (center) forms a 3c-2e (three-center two-electron) C−H−B bond which may facilitate the transfer of a hydrogen from the ring to rhodium when reacted with Cp*Li.

In a study of Ziegler−Natta catalysis polymerization using Cp_2TiH^+ plus ethene as a model, Sakai[47] considered the insertion reaction of the metal hydride to form the $Cp_2TiC_2H_5^+$ species. As seen from eq 1, the complex, transition state, and product relative enthalpies (kcal/mol) for $CpFeH^+$ and Cp_2TiH^+ are very similar.

$$\begin{array}{cccc} CpM(H)^+ + C_2H_4 \rightarrow & \text{complex} \rightarrow & \text{TS} & \rightarrow CpMC_2H_5^+ \\ M = Fe\ 0.0 & -42.7\ (\mathbf{7}) & -43.2 & -52.4\ (\mathbf{9}) \\ M = CpTi\ 0.0 & -33.5 & -34.3 & -55.1 \end{array} \qquad M = Fe, CpTi \quad (1)$$

Both $CpFe(H)C_2H_4^+$, a 15-electron system, and $Cp_2Ti(H)C_2H_4^+$, a 16-electron system, rearrange with a barrier that is negative after zero-point corrections.

Bärsch et al.[33] have also calculated a similar β-hydrogen transfer to a SiH_3 ligand (eq 3). The barrier for eq 2 is significantly lower than for eq 3.

$$CpFeC_2H_5^+ (\mathbf{9}) \rightarrow C_5H_6FeC_2H_4^+ (\mathbf{7}) \quad \Delta H^{\ddagger} = 9.7\ \text{kcal/mol} \quad (2)$$

$$SiH_3FeC_2H_5^+ \rightarrow SiH_4FeC_2H_4^+ \quad \Delta H^{\ddagger} = 29.2\ \text{kcal/mol} \quad (3)$$

In a study of ethane polymerization with the catalyst $[MLL'R]^+$ M = Ti, V, Cr, and Mn, Schmid and Ziegler[48] considered the β-hydrogen transfer reaction between the C_2H_5 and C_2H_4 ligands. This reaction step can be compared to the ligand-to-ligand transfer which occurs in essentially one step along the reaction path **TS7/8** → **8** → **TS8/9**. In both reaction

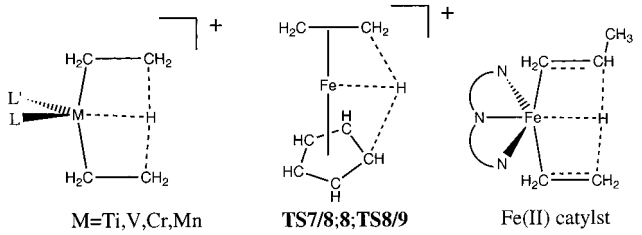

steps, the hydrogen that transfers has a strong interaction with the transition metal center. The activation barriers are between 10 and 20 kcal/mol depending on the system. In a study of the bis(imino)pyridyl−Fe(II) olefin polymerization catylst (see above), Morokuma and co-workers[49] calculated (B3LYP/BSIII//B3LYP/BSI) a barrier on the triplet spin-state surface of 7.5 kcal/mol (ΔH_a(298K)) for the ligand-to-ligand hydrogen transfer from L = C_3H_7 to L′ = C_2H_4.

The $CpFeC_2H_5^+$ complex **9** is 2.1 kcal/mol less stable than **7**. A barrier of 27.0 kcal/mol (**TS9/10**) separates **9** from $C_2H_5-C_5H_5Fe^+$ **10**, which is 14.2 kcal/mol higher the corresponding barrier between **3** and **4**. The difference between the two barriers (**9**→**10** and **3**→**4**) can be attributed to the weaker binding of Fe^+ to **10** (−67.0 kcal/mol) compared to **4** (−87.3 kcal/mol). The binding energy of Fe^+ to $C_2H_5-C_5H_5$ is 13.3 kcal/mol greater than to C_5H_6 (see eqs 4 and 5) which can be attributed to the fact that the attractive interactions between Fe^+ and the ethyl substituent exceed the increase in strain energy induced in the ligand.

$$Fe^+ + C_5H_6 \rightarrow C_5H_6Fe^+ \quad \Delta H_{rxn} = -53.7\ \text{kcal/mol} \quad (4)$$

$$Fe^+ + C_2H_5-C_5H_6 \rightarrow C_2H_5-C_5H_5Fe^+ (\mathbf{10}) \quad \Delta H_{rxn} = -67.0\ \text{kcal/mol} \quad (5)$$

In a communication, Bowers and co-workers[50] reported experimental and computational evidence that the Cp ligand participates directly in the mechanism of C−H bond activation in methane by $CoCp^+$. In their proposed mechanism (see below),

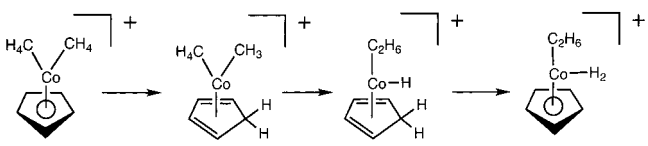

a ligand-to-ligand hydrogen transfer occurs between coordinated CH_4 and the Cp ring.

(46) Ginsberg, A.; Pritzkow, H.; Siebert, W. *J. Organomet. Chem.* **2001**, *619*, 7.
(47) Sakai, S. *THEOCHEM* **2001**, *540*, 157.
(48) Schmid, R.; Ziegler, T. *Organometallics* **2000**, *19*, 2756.
(49) Khoroshun, D. V.; Musaev, D. G.; Vreven, T.; Morokuma, K. *Organometallics* **2001**, *20*, 2007.
(50) Carpenter, C. J.; van Koppen, P. A. M.; Bowers, M. T. *J. Am. Chem. Soc.* **2000**, *122*, 392.

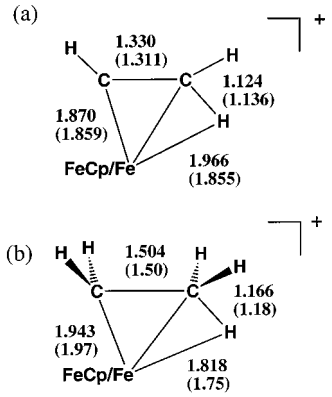

Figure 5. (a) Comparison of the structural parameters of the $FeC_2H_3^+$ complex in the higher-energy triplet state with the $CpFeC_2H_3^+$ complex (in parentheses). (b) Comparison of the structural parameters of the $FeC_2H_5^+$ complex in the higher-energy triplet state with the $CpFeC_2H_5^+$ complex (in parentheses).

Migration of an alkyl group from iron to a Cp ring has been observed by Blaha et al.[51a] and Carpenter et al.[51b] However, these authors proposed a dissociative mechanism because the alkyl group has an *exo*-relationship in the product. More recently, Bleuel et al.[51c] obtained evidence for the concerted addition of an alkyl group to a cyclopentadienyl ring in a rhodium system, similar to that calculated for **9** → **10**. In their mechanism, which was derived from deuterium labeling, a $CpRh(PR_3)(Cl)R \rightarrow R{-}C_5H_5Rh(PR_3)(Cl)$ step was proposed.

It is worth pointing out that the $FeC_2H_3^+$ and $FeC_2H_5^+$ complexes differ significantly from the $CpFeC_2H_3^+$ (**3**) and $CpFeC_2H_5^+$ (**9**) complexes. Chen et al.,[35] using B3LYP density functional theory with a cc-pVTZ basis set on C and H and a (8s/6p/4d/1f) contraction on iron, found that the lowest quintet state of $FeC_2H_3^+$ was 17.9 kcal/mol below the lowest-energy triplet structure. The quintet structure featured an Fe−C σ bond (1.923 Å) and no agostic interaction with the β-hydrogen. However, it is the higher-energy $FeC_2H_3^+$ triplet structure which bears the much closer resemblance to $CpFeC_2H_3^+$ (Figure 5). When the wave functions of triplet/quintet $FeC_2H_3^+$ and $CpFeC_2H_3^+$ were analyzed, the Fe−C bond in quintet $FeC_2H_3^+$ was found to have significant s-character while in triplet $FeC_2H_3^+$, the 4s orbital was empty. The agostic interaction with the β-hydrogen is characterized by significant donation from the CH σ bond into the empty Fe 4s orbital. In the $CpFeC_2H_3^+$ complex (**3**), the Cp ring disfavors the occupation of 4s orbitals which can then act as the acceptor orbital in an agostic interaction.

Fiedler et al.[36] used B3LYP density functional theory with a DZP basis set on C/H and a (8s5p3d) contraction on Fe to optimize a classical quintet ($^5A'$) $FeC_2H_5^+$ structure (Fe−C 1.98 Å) and a nonclassical triplet ($^3A'$) structure (14 kcal/mol higher in energy) which is characterized by an agostic interaction to the β-hydrogen (Fe−H 1.75 Å). Again, the $CpFeC_2H_5^+$ complex (**9**) is very similar to the low-spin triplet $FeC_2H_5^+$ (Figure 5) rather than the high-spin form.

Hill et al.[52] calculated the stable alkyl complex $CpFe(CO)_2C_2H_5$ and the β-elimination product, $CpFe(CO)(H)C_2H_4$ at the B88LYP level. In contrast to $CpFeC_2H_5^+$ (**9**), the C_2H_5 ligand in $CpFe(CO)_2C_2H_5$ is σ-bonded rather than π-bonded to iron which may be due to greater steric repulsion around the transition metal center. The C═C distance of the ethene ligand in $CpFe(CO)(H)C_2H_4$ (1.43 Å) is longer than that calculated for $CpFe(H)C_2H_4$ (**8**) (1.387 Å) which may indicate stronger π coordination compared to **8**. The calculated Fe−H distance in $CpFe(CO)(H)C_2H_4$ (1.52 Å) and **8** (1.526 Å) are both very similar.

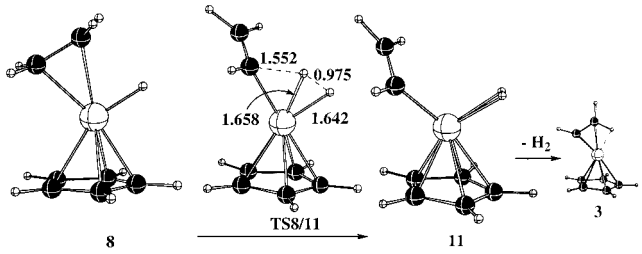

Figure 6. Molecular plots of species optimized at the B3LYP/6-31G-(d) level. The reaction profile with energies in kcal/mol relative to C_5H_6-$FeC_2H_4^+$ (**7**) is given in Scheme 2b.

2a. Dehydrogenation of $C_5H_6FeC_2H_4^+$. Dehydrogenation/hydrogenation reactions are important catalytic steps in many transition metal reactions. After much searching, the dehydrogenation of $C_5H_6FeC_2H_4^+$ **7** was found to occur in two steps (Scheme 2b, Figure 6). First, the hydrido species **8** is formed. Breaking a second C−H bond and forming the second Fe−H bond (**TS8/11**) requires the input of an additional 33.1 kcal/mol of activation. The C−H distance is 1.552 Å in the transition state while the Fe−H distance is 1.658 Å. Also, the transition state shows the formation of a dihydrogen complex rather than a dihydrido complex as the H−H distance is 0.975 Å; albeit with a lengthened H−H bond due to interaction with the metal. The $CpFe(H_2)C_2H_3^+$ intermediate **11** is 8.6 kcal/mol lower than **TS8/11** where the most interesting feature is the C_2H_3 ligand which is σ-bonded to the metal rather than π-bonded as found in $CpFeC_2H_3^+$ **3**.

The dehydrogenation reaction path was considered at the B3LYP/DZP level for $FeC_2H_6^+$ by Holthausen et al.[37] (eq 6). The reaction (eq 6) takes place with quartet spin multiplicity where two hydrogen atoms are transferred sequentially to the iron center to form the dihydrogen $Fe(H_2)C_2H_4^+$ complex. The sequence of steps is very similar in eq 7, where $CpFeC_2H_5^+$ (**9**) transfers two hydrogens to form $CpFe(H_2)C_2H_3^+$ (**11**). The overall barrier is also very similar (40 kcal/mol, eq 6; 42.8 kcal/mol, eq 7).

$$FeC_2H_6^+ \rightarrow FeC_2H_4^+ + H_2 \quad (6)$$

$$CpFeC_2H_5^+ \,(\mathbf{9}) \rightarrow (\mathbf{8}) \rightarrow (\mathbf{11}) \rightarrow CpFeC_2H_3^+ \,(\mathbf{3}) + H_2 \quad (7)$$

2b. Hydrogenation of NBD-Fe^+. Hydrogenation of NBD to NBN (Figure 7) can be catalyzed by several transition metal systems including RhL^+, L = PPh_3;[53] and $M(CO)_3$, (M = Cr, Mo, W).[54,55] In the $RhPPh_3^+$ system, H_2 oxidatively adds to $Rh(\eta^4\text{-NBD})(PPh_3)_2$ to form a dihydrido complex $Rh(H)_2(\eta^4\text{-NBD})(PPh_3)_2$ which loses one PPh_3 and then hydrogenates NBD to NBN. The $M(CO)_3$ (M = Cr, Mo, W) system is photocatalytic, where H_2 adds to $M(\eta^4\text{-NBD})(CO)_3$ to form the nonclas-

(51) (a) Blaha, J. P.; Wrighton, M. S. *J. Am. Chem. Soc.* **1985**, *107*, 2694. (b) Carpenter, N. E.; Khan, M. A.; Nicholas, K. M. *Organometallics* **1999**, *18*, 1569. (c) Bleuel, E.; Schwab, P.; Laubender, M.; Werner, H. *J. Chem. Soc., Dalton Trans.* **2001**, 266.

(52) Hill, R. O.; Marais, C. F.; Moss, J. R.; Naidoo, K. J. *J. Organomet. Chem.* **1999**, *587*, 28.

(53) Esteruelas, M. A.; Herrero, J.; Martín, M.; Oro, L. A.; Real, V. M. *J. Organomet. Chem.* **2000**, *599*, 178.

(54) (a) Jackson, S. A.; Hodges, P. M.; Poliakoff, M.; Turner, J. J.; Grevels, F.-W. *J. Am. Chem. Soc.* **1990**, *112*, 1221. (b) Childs, G. I.; Cooper, A. I.; Nolan, T. F.; Carrott, M. J.; George, M. W.; Poliakoff, M. *J. Am. Chem. Soc.* **2001**, *123*, 6857.

(55) Chmielewski, D.; Grevels, F.-W.; Jacke, J.; Schaffner, K. *Angew. Chem., Int. Ed. Engl.* **1991**, *30*, 1343.

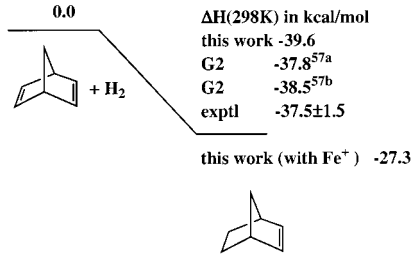

Figure 7. Reaction profile comparing the hydrogenation of NBD by theory and experiment (see ref 57). The Fe^+-catalyzed reaction is less exothermic (−27.3 kcal/mol) because the reactant is η^4-complexed to Fe^+, while the product is η^2-complexed to Fe^+.

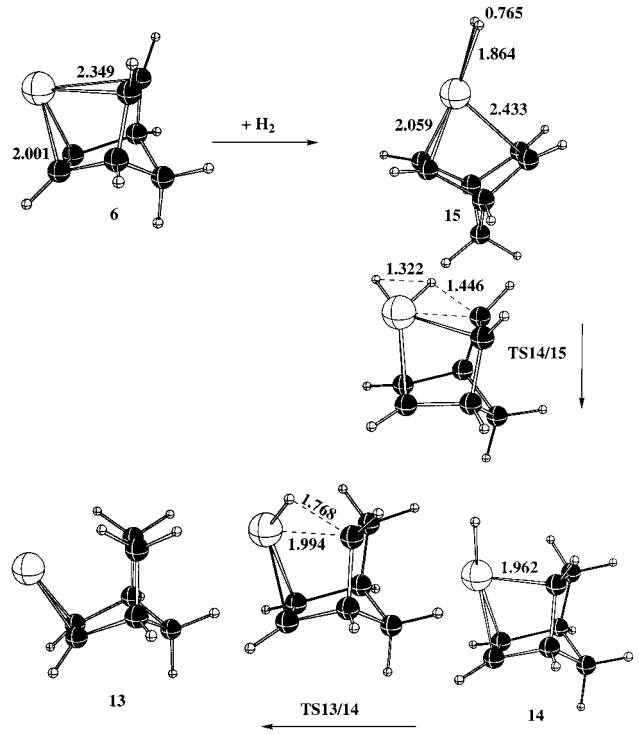

Figure 8. Molecular plots of species optimized at the B3LYP/6-31G-(d) level for hydrogenation of NBD. The reaction profile with energies in kcal/mol relative to $C_5H_6FeC_2H_4^+$ (**7**) is given in Scheme 3.

Scheme 3

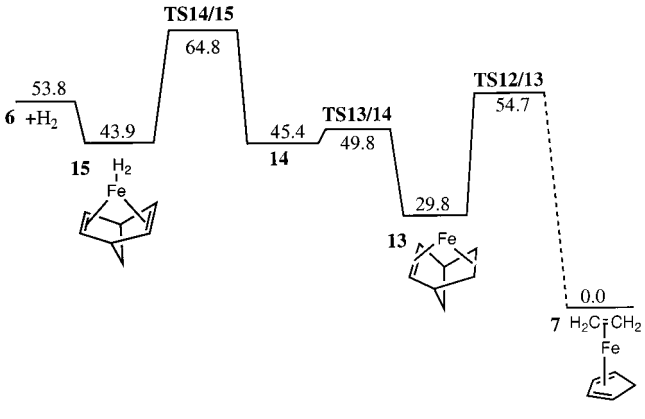

sical dihydrogen complex M(η^2-H_2)(η^4-NBD)$(CO)_3$ (M = Cr, Mo, W) which then hydrogenates NBD to NBN. When dideuterium is used, Cr(η^2-D_2)(η^4-NBD)$(CO)_3$ leads to formation of *endo*-[D_2]NBN.

The calculated Fe^+-catalyzed NBD hydrogenation to NBN (Scheme 3 and Figure 8) begins with the coordination of dihydrogen to $C_7H_8Fe^+$ (**6**) to form $C_7H_8Fe(H_2)^+$ (**15**). The dihydrido complex was considered, but only the dihydrogen species exists on the potential energy surface. This same conclusion was reached by previous workers in the study of $CH_2Fe(H_2)^+$ and $C_2H_4Fe(H_2)^+$,[37,38] where it was pointed out that the high formal oxidation state of iron might disfavor the dihydrido form.[38,56] In both $C_7H_8Fe^+$ (**6**) and $C_7H_8Fe(H_2)^+$ (**15**), the iron is asymmetrically coordinated between the two double bonds. The two pairs of Fe−C distances of 2.001 and 2.349 Å in **6** increase slightly to 2.059 and 2.433 Å when H_2 coordinates in **15**. The H_2 ligand in **15** bisects the molecular plane with Fe−H distances of 1.864 Å and a H−H distance of 0.765 Å. The first hydrogen is transferred to carbon in **TS14/15** with a forming C−H distance of 1.446 Å and a breaking H−H distance of 1.322 Å. The hydrido intermediate **14** has a very short Fe−C bond (1.962 Å) to the other half of the hydrogenated C=C double bond and has some similarity to an FeH^+-substituted NBN where the FeH^+ group interacts with the remaining C=C double bond. From **14**, there is a very small barrier (4.4 kcal/mol) for transferring the second hydrogen. The breaking Fe−C bond increases only slightly (1.962 → 1.994 Å) while the interaction with the C=C double bond increases. The overall exothermicity of the uncatalyzed reaction is 37.5 ± 1.5 kcal/mol by experiment or high-level theory.[57] With Fe^+ coordinated to reactant and product, the exothermicity decreases to 14.1 kcal/mol because Fe is η^4 in the reactant and η^2 in the product. With respect to $C_7H_8Fe^+$ plus H_2, the activation barrier is 11.0 kcal/mol, which increases to 20.9 kcal/mol when the H_2 binding energy in included. The computed mechanism is consistent with the addition of both hydrogens to *endo* positions of NBN.

The dehydrogenation transition state (**TS14/15**) is compared to the calculated transition state for dehydrogenation of $HFeC_2H_5^+$ in Figure 9. The similarity of the structures is very clear; where two C−H bonds are replaced by C−C bonds in **TS14/15** and the iron is interacting with a π bond. The H−H bond is broken to a much smaller extent in **TS14/15** compared to the $HFeC_2H_5^+$ → $Fe(H_2)C_2H_4^+$ transition state.

3. Hydrogen/Deuterium Scrambling in $C_5H_6Fe/C_2D_4^+$. The addition of dideuterium to $C_5H_6Fe^+$ is known to scramble hydrogen and deuterium.[58] One hydrogen is known to be exchanged more rapidly (eq 8) than the other five. The slow exchange is thought to involve a 1,2-*exo* hydrogen migration in the cyclopentadiene ligand. The experimental activation barrier for 1,2-hydrogen migration in uncomplexed cyclopentadiene is 23.6 kcal/mol.[59]

$$C_5H_6Fe^+ + D_2 \rightarrow C_5H_6Fe(D_2)^+ \rightarrow C_5H_5FeH(D_2)^+ \rightarrow C_5H_5FeD(HD)^+ \rightarrow C_5H_5DFe(HD)^+ \quad (8)$$

For hydrogen/deuterium scrambling in the $C_5H_6Fe^+/D_2$ system (Scheme 4a), the activation barrier for the first H/D exchange is 14.2 kcal/mol and the barrier for additional H/D exchanges is 23.6 kcal/mol.[58] In the $C_5H_6Fe^+/C_2D_4$ system (Scheme 4a), the overall reaction profile is similar but the details are different. First, the binding energy of ethene is much greater than dihydrogen (51.3 vs 14.2 kcal/mol). Second, the hydrido species exists for $CpFe(H)D_2^+$, but not for $CpFe(H)C_2D_4^+$. Third, the 1,2-hydrogen migration barrier is greater than the ligand binding enthalpy for $C_5H_6Fe^+/D_2$, but less than the ligand binding enthalpy for $C_5H_6Fe^+/C_2D_4$. Thus, multiple H/D exchanges should occur more readily in the $C_5H_6Fe^+/C_2D_4$ system relative to the $C_5H_6Fe^+/D_2$ system.

4. $CpFeR^+$ (R=C_2H_2, C_2H_3, C_2H_4, C_2H_5) versus $C_5H_6FeR^+$ (R=C_2H_2, C_2H_4). When the quartet complex $C_5H_6FeC_2H_2^+$ was optimized in C_s symmetry (**1′**) (Figure 10), a force constant

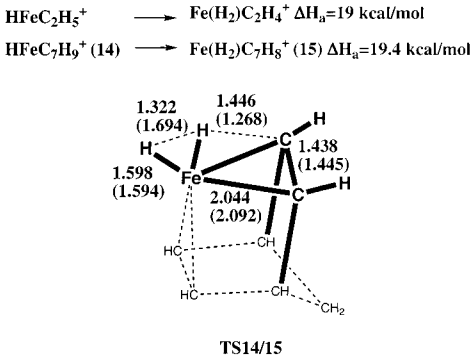

Figure 9. The structural parameters for dehydrogenation of NBN (values in parentheses) are very similar to dehydrogenation of $FeC_2H_6^+$ (see ref 37). In the drawing, the transition state for dehydrogenation of $FeC_2H_6^+$ is shown by bold lines where the two downward-pointing lines are terminated by hydrogen atoms.

calculation revealed one imaginary frequency. When re-optimized in C_1 symmetry (**1**), a distorted structure was obtained with no imaginary frequencies. However, the distortion, which caused the Fe−C distances to the C_5H_6 ring to become asymmetric, lowered the energy by much less than 0.1 kcal/mol. In the $C_5H_6FeC_2H_4^+$ complex, the C_s structure (**7′**) was also a transition state to a C_1-symmetry complex (**7**), 4.1 kcal/mol lower in energy. An analysis of the wave functions indicates that the distortions in **7** are due to the rehybridization of the 4s orbital on iron with a d-orbital to generate new orbitals that overlap more effectively with those in the C_2H_4 ligand. Thus there is a compromise between the best orbitals for interacting with the C_5H_6 ring and the attached C_2H_4 ligand.

Table 4. Calculated B3LYP/6-31G(d) Bond Enthalpy (kcal/mol) at 298 K for Breaking R−C Bond

	R = $CpFe^+$; R′= H	R = H; R′= H	R = H; R′= $CpFe^+$
R−CH_2CH_2−R′	55.6	100.1	52.0
R−CH_2CH−R′	43.2	39.6	90.3
R−CHCH−R′	62.0	109.1	57.5
R−CHC−R′	46.8	42.3	

The bond enthalpies for R−$CpFe^+$, R = C_2H_5, C_2H_4, C_2H_3, and C_2H_2 are given in Table 4. In addition, the bond enthalpies for breaking a C−H bond in C_2H_6, C_2H_5, C_2H_4, and C_2H_3 are compared with the C−H bond enthalpies in $CpFeC_2H_5^+$, $CpFeC_2H_4^+$, and $CpFeC_2H_3^+$. The $FeC_7H_7^+$ and $FeC_7H_9^+$ cations are considered, even though they are not involved in the retrocyclization reactions, to extend the range of comparison. In contrast to the C−H bond energies of C_2H_n−H (n = 5−2), where the C−H bond in C_2H_6 and C_2H_4 (100.1 and 109.1 kcal/mol) is much stronger than in C_2H_5 and C_2H_3 (39.6 and 42.3 kcal/mol), the R−$FeCp^+$ bond energies span a smaller range (43.2−62.0 kcal/mol). While C_2H_5 and C_2H_3 gain a π-bond when the C−H bond is broken, in $CpFeC_2H_5^+$ and $CpFeC_2H_3^+$ removing the R group requires the additional loss of an agostic interaction. In the series $CpFeC_2H_n^+$−H (n = 4−2), the C−H bond in $CpFeC_2H_4^+$ (90.3 kcal/mol) is much stronger than in

Scheme 4

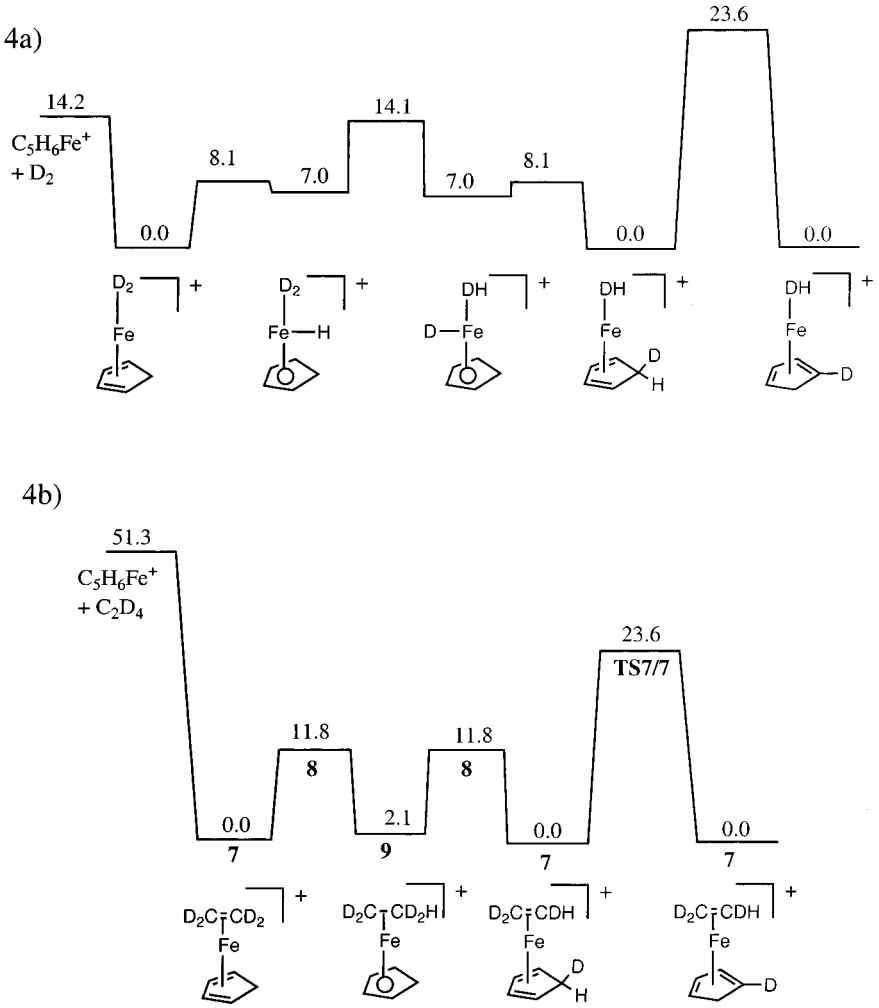

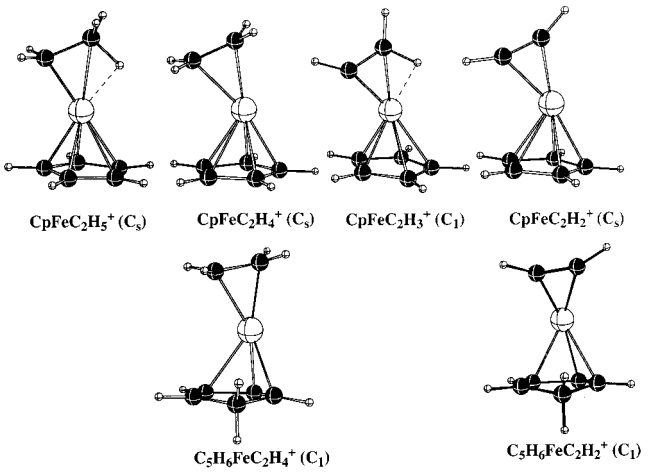

Figure 10. Molecular plots of C_2H_5, C_2H_4, C_2H_3, and C_2H_2 complexed to $CpFe^+$ and C_2H_5 and C_2H_4 complexed to $C_5H_6Fe^+$ optimized at the B3LYP/6-31G(d) level.

$CpFeC_2H_5$ or $CpFeC_2H_3^+$ (52.0, 57.5 kcal/mol) which reflects the strong binding of the ethene group. The binding of C_2H_4 and C_2H_2 is stronger to $C_5H_6Fe^+$ (51.3 and 56.8 kcal/mol) than to $CpFe^+$ (43.2 and 46.8 kcal/mol) which is due to the weaker binding of Fe^+ to C_5H_6 compared to C_5H_5 (53.7 and 86.7 kcal/mol; Table 3).

5. CID of $C_5H_6Fe^+ + C_2H_4$ and C_2H_2. Rearrangements of $C_5H_6Fe^+$ plus substrates can be studied by allowing the cation to react with a variety of isomers and comparing the CID plots. When the same CID plot results from different substrates, this indicates that rearrangement has occurred to form a common intermediate, where the intensity pattern of fragments can give clues to the structure of the intermediate.

In the reaction of small alkenes and alkynes with $C_5H_6Fe^+$ using Fourier transform ion cyclotron resonance (FTICR) mass spectrometry, the main process involves loss of H or H_2 to generate a complexes whose structure can be probed by CID (eq 9−12).

$$C_5H_6Fe^+ + C_2H_2 \rightarrow FeC_7H_7^+ + H \quad (9)$$

$$C_5H_6Fe^+ + C_2H_4 \rightarrow FeC_7H_8^+ + H_2 \quad (10)$$

$$C_5H_6Fe^+ + HC{\equiv}CCH_3 \rightarrow FeC_8H_8^+ + H_2 \quad (11)$$

$$C_5H_6Fe^+ + H_2C{=}CHCH_3 \rightarrow FeC_8H_{10}^+ + H_2 \quad (12)$$

In the reaction between $C_5H_6Fe^+ + C_2H_4$, four possible structures were considered for the $FeC_7H_8^+$ complex (a−d). The CID of the reaction of Fe^+ with cycloheptatriene (a) showed a different pattern from the CID of eq 10 while (b) could be eliminated due to incompatible fragmentation pathways. Structure (d) was excluded by consideration of earlier work by Bakhtiar and Jacobson.[21] Chen et al.[20] settled on (c) as the identity of $FeC_7H_8^+$ in eq 10. However, the present calculations suggest that (e) should be considered as a strong candidate. First, the reaction to (c) plus H_2 is endothermic by 5.8 kcal/mol, while the reaction to (e) plus H_2 is exothermic by 15.8 kcal/mol. Second, the activation barrier to (c) plus H_2 is 9.8 kcal/mol greater than the barrier to (e) plus H_2.

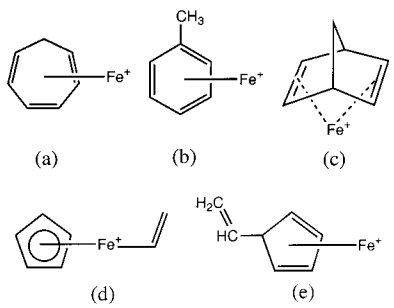

Conclusions

The retro Diels−Alder reaction of norbornadiene catalyzed by Fe^+ has an activation barrier that is 3.1 kcal/mol lower than that of the concerted uncatalyzed reaction. In contrast, the Fe^+-catalyzed retrocyclization of norbornene has a higher activation barrier than the concerted reaction. In both reactions, a bicyclic metallocycle is formed. Ligand-to-ligand hydrogen migrations in $C_5H_6FeC_2H_2^+$ and $C_5H_6FeC_2H_4^+$ lead to $CpFeC_2H_3^+$ and $CpFeC_2H_5^+$, respectively, in near-thermoneutral reactions that have low activation barriers. A pathway for dehydrogenation of $C_5H_6FeC_2H_4^+$ has been calculated leading to $C_5H_6FeC_2H_3^+$ with a 44.9 kcal/mol activation barrier. In addition, the hydrogenation norbornadiene is predicted to proceed with a stepwise mechanism and 20.9 kcal/mol activation barrier. While there is no evidence for a dihydrido intermediate, a monohydrido intermediate is predicted in both mechanisms. In hydrogen/deuterium exchange for $C_5H_6Fe/C_2D_4^+$, the first exchange occurs with facile formation of a $CpFeC_2D_4H^+$ intermediate. Subsequent H/D exchanges require 1,2-hydrogen migrations in the complexed cyclopentadiene of $C_5H_5DFeC_2D_3H^+$ which has a calculated barrier of 23.6 kcal/mol. When comparing binding energies of $R-C_2H_2$, $R-C_2H_3$, $R-C_2H_4$, and $R-C_2H_5$ ($R = CpFe^+$ or H), the binding of $CpFe^+$ ($R = CpFe^+$) to C_2H_2 and C_2H_4 is greater than the C−H bond energy in C_2H_3 and C_2H_5, while the binding of $CpFe^+$ ($R = CpFe^+$) to C_2H_3 and C_2H_5 is less than the C−H bond energy in C_2H_4 and C_2H_6.

Acknowledgment. Computer time was provided by the Alabama Supercomputer Network and the Maui High Performance Computer Center. M.L.M. thanks Sun Microsystems Computer Corporation for the award of an Academic Equipment Grant.

JA011165Q

(56) For additional work concerning dihydrogen and dihydride transition metals see: (a) Crabtree, R. H. *Acc. Chem. Res.* **1990**, *23*, 95. (b) *Transition Metal Hydrides*; Dedieu, A., Ed.; VCH: New York, 1992. (c) Bautista, M. T.; Cappellani, E. P.; Drouin, S. D.; Morris, R. H.; Schweitzer, C. T.; Sella, A.; Zubkowski, J. *J. Am. Chem. Soc.* **1991**, *113*, 4876. (d) Lin, Z.; Hall, M. B. *J. Am. Chem. Soc.* **1992**, *114*, 6102. (e) Hills, A.; Hughes, D. L.; Jimenez-Tenorio, M.; Leigh, G. J.; C. McGeary, A.; Rowley, A. T.; Bravo, M.; McKenna, C. E.; McKenna, M. J. *Chem. Soc. Chem. Commun.* **1991**, 522. (f) Hills, A.; Hughes, D. L.; Jimenez-Tenorio, M.; Leigh, G. J.; Rowley, A. T. *J. Chem. Soc., Dalton Trans.* **1993**, 3041. (g) Hills, A.; Hughes, D. L.; Jimenez-Tenorio, M.; Leigh, G. J.; Rowley, A. T. *J. Chem. Soc., Dalton Trans.* **1993**, 3041. (h) Landis, C. R.; Brauch, T. W. *Inorg. Chim. Acta* **1998**, *270*, 285. (i) Bautista, M. T.; Cappellani, E. P.; Drouin, S. D.; Morris, R. H.; Schweitzer, C. T.; Sella, A.; Zubkowski, J. *J. Am. Chem. Soc.* **1991**, *113*, 4876. (j) Bayse, C. A.; Hall, M. B.; Pleune, B.; Poli, R. *Organometallics* **1998**, *17*, 4309. (k) Jia, G.; Lau, C. P. *Coord. Chem. Rev.* **1999**, *190*−*192*, 83. (l) Helleren, C. A.; Henderson, R. A.; Leigh G. J. *J. Chem. Soc., Dalton Trans.* **1999** 1213. (m) Maseras, F.; Lledós, A.; Clot, E.; Eisenstein, O. *Chem. Rev.* **2000**, *100*, 601. (n) Soubra, C.; Oishi, Y.; Albright, T. A.; Fujimoto, H. *Inorg. Chem.* **2001**, *40*, 620.

(57) (a) Rogers, D. W.; McLafferty, F. J. *J. Phys. Chem. A* **1999**, *103*, 8733. (b) Castaño, O.; Notario, R.; Abboud, J.-L. M.; Gomperts, R.; Palmeiro, R.; Frutos, L.-M. *J. Org. Chem.* **1999**, *64*, 9015.

(58) McKee, M. L. *Int. J. Mass Spectrom.* **2000**, *201*, 143.

(59) (a) Spangler, C. W. *Chem. Rev.* **1976**, *76*, 187. (b) Roth, W. *Tetrahedron Lett.* **1964**, 1009. (c) Berson, J. A.; Aspelin, G. G. *Tetrahedron* **1964**, *20*, 2697.